

USP35 promotes hepatocellular carcinoma progression by protecting PKM2 from ubiquitination-mediated degradation

TAO LV^{1,2}, BO ZHANG³, CHENGHAO JIANG^{1,2}, QIWEN ZENG¹, JIAYIN YANG^{1,2} and YONGJIE ZHOU¹

¹Laboratory of Liver Transplantation, Frontiers Science Center for Disease-Related Molecular Network;
Departments of ²Liver Transplantation and ³Critical Care Medicine, West China Hospital of
Sichuan University, Chengdu, Sichuan 610041, P.R. China

Received November 27, 2022; Accepted June 30, 2023

DOI: 10.3892/ijo.2023.5561

Abstract. Hepatocellular carcinoma (HCC) is the most frequently diagnosed primary liver cancer with a high mortality rate and imposes a huge burden on patients and society. Recently, ubiquitin-specific protease 35 (USP35) was found to be involved in cell proliferation and mitosis, but its role in HCC remains largely unknown. The expression of USP35 in HCC and its association with patient prognosis in the study cohort and public databases was analyzed in the present study. The effects of USP35 on the malignant biological behavior of HCC were analyzed by cellular functional experiments. Mechanistically, the effect of USP35 deubiquitylation on the M2 splice isoform of pyruvate kinase (PKM2) and on the Warburg effect of tumor cells were verified by western blotting and ubiquitination assay. The results of the present study demonstrated that USP35 is highly expressed in HCC and its high expression is significantly associated with poor prognosis of patients with HCC. In the present study, it was also demonstrated that inhibiting the expression of USP35 can impair the malignant properties (proliferation, migration and invasion) of HCC tumor cells by elevating the ubiquitination level of PKM2, the deubiquitinated form of which is critical for glycolysis in tumor cells. The present study therefore indicated that USP35 may be a target in the treatment of HCC.

Introduction

Primary liver cancer can be divided into hepatocellular carcinoma (HCC), bile duct cell carcinoma and mixed cell carcinoma, among which HCC accounts for >80% of primary liver cancer cases (1). Globally, liver cancer is the fourth most common cause of cancer-related death and ranks sixth in cancer incidence (2). According to the annual forecast by the World Health Organization, it is estimated that >1 million patients will die of liver cancer in 2030 (3). In the United States, from 2000 to 2016, the mortality rate of liver cancer increased by 43% (from 7.2 cases per 100,000 to 10.3 cases per 100,000), and the 5-year survival rate was 18% (4). Liver cancer has become the fourth most lethal cancer, after pancreatic cancer (5).

HCC can occur in patients with chronic liver diseases, such as hepatitis B or hepatitis C or those patients suffering from alcohol abuse (6). Patients with chronic liver diseases exhibit persistent liver inflammation, progressive liver fibrosis and abnormal regeneration of hepatocytes (6). These abnormal physiological processes eventually lead to cirrhosis and a series of genetic and epigenetic alterations, which ultimately contribute to the formation of dysplastic nodules (precancerous lesions) (7). Another abnormal physiological processes can then enable dysplastic cells to gain the advantages of proliferation, invasion and survival, and completely transform into mature HCC (8). Somatic mutation analysis can be used to determine the target pathway of telomerase, which can maintain telomeres by increasing telomerase activity and preventing telomere shortening and replication attenuation (7). These changes occur in the early stage of tumor occurrence. Hot spot mutations in the telomerase reverse transcriptase (TERT) promoter have been found in dysplastic nodules of liver cirrhosis (8). With the increase in the degree of atypical hyperplasia, the TERT mutation frequency has also increased: 6% in low grade dysplastic nodules, 19% in high grade dysplastic nodules and 60% in early HCC. In chronic liver disease, inflammation is related to the increase of oxidative stress in liver parenchyma. The activation of nuclear factor erythroid 2 related factor 2 and kelch-like ECH-related protein 1 signaling pathways stimulate the protective effect from oxidation at the cellular level (7,8). Inactivating mutations in the tumor suppressor gene, TP53, occur in 20-50% of HCC cases and these mutations may interfere with the

Correspondence to: Dr Yongjie Zhou, Laboratory of Liver Transplantation, Frontiers Science Center for Disease-Related Molecular Network, West China Hospital of Sichuan University, 37 Guoxue Alley, Wuhou, Chengdu, Sichuan 610041, P.R. China
E-mail: yongjiezhou@scu.edu.cn

Dr Jiayin Yang, Department of Liver Transplantation, West China Hospital of Sichuan University, 37 Guoxue Alley, Wuhou, Chengdu, Sichuan 610041, P.R. China
E-mail: doctoryjy@scu.edu.cn

Key words: ubiquitin-specific protease 35, hepatocellular carcinoma, M2 splice isoform of pyruvate kinase, ubiquitination

cell cycle (7,8). At present, non-alcoholic fatty liver disease (NAFLD) has become the main cause of HCC in many countries (9). The majority of risk factors associated with NAFLD are also independently associated with HCC including obesity, diabetes and genetic polymorphisms of patatin-like phospholipase domain containing 3, transmembrane 6 superfamily 2 and glucokinase regulator. Fat toxicity and DNA oxidative damage associated with steatosis can induce liver carcinogenesis (10). Therefore, it is urgent to explore the key factors that regulate the malignant progression of HCC.

Ubiquitin is a small protein composed of 76 amino acids with a molecular weight of ~8.5 kDa (11), and the highly conserved ubiquitin protein is widely distributed in all eukaryotic cells. Ubiquitination refers to the process by which ubiquitin is attached to proteins in cells during catalysis by a series of enzymes, which selectively modify target proteins (12). This process typically requires the cooperation of three ubiquitination enzymes: E1 ubiquitin activating enzyme, E2 ubiquitin binding enzyme and E3 ubiquitin ligase (13). Similar to other posttranslational modifications, ubiquitination is reversible and can be reversed by a large group of proteases termed deubiquitinases (DUBs) (14). Most DUBs cleave and release ubiquitin from substrate proteins, edit ubiquitin chains and process ubiquitin precursors (14). As a ubiquitin-specific protease, USP35 plays an important role in regulating the deubiquitination of proteins. USP35 interacts with ferritin (FPN) and functions as a deubiquitinating enzyme to maintain FPN protein stability and further regulate ferroptosis in lung cancer cells (15). In ovarian cancer, USP35 can directly deubiquitinate and inactivate the stimulator of interferon genes protein, decreasing the sensitivity of tumor cells to cisplatin (16). However, whether USP35 plays a role in the malignant biological progression of HCC remains unknown.

The present study aimed to analyze the expression of USP35 in patients with HCC and the correlation between USP35 expression and HCC prognosis, to investigate the role of USP35 in HCC malignant progression, and to preliminarily explore the underlying molecular mechanism of USP35 in HCC.

Materials and methods

Patients and samples. In total, 96 patients (age range, 29-74 years; mean age, 53 years old) with HCC were enrolled from the Department of Liver Surgery at West China Hospital of Sichuan University (Chengdu, China) from March 2015 to May 2019. All studies were approved by The Ethics Committee of the West China Hospital (Chengdu, China; approval no. 20150176). All patients involved in the present study provided signed written informed consent. The primary cancer tissues and the paired normal adjacent tissues were immediately snap-frozen in liquid nitrogen and stored in liquid nitrogen until use for mRNA and protein analyses.

The specific inclusion criteria were as follows: i) HCC was confirmed through pathological testing after surgical resection of the tumor; ii) the patient was diagnosed with HCC for the first time; iii) the patient did not receive any treatment before the surgery; iv) the patient had not been diagnosed with other serious malignant diseases; v) the various clinical data of the patient was complete; and vi) the prognosis follow-up data of the patient was available and not missing.

The exclusion criteria were as follows: i) The patient had a communication disorder and could not communicate effectively; ii) the heart, brain, lung or kidney of the patient had organic dysfunction; iii) patients diagnosed with HCC for the first time but with distant metastasis; iv) the clinical data of the patient was incomplete; v) the patient had systemic diseases; vi) the patient had autoimmune dysfunction; and vii) the follow-up data for patient prognosis was incomplete.

Cell culture. HCC cell lines, Hep3B, Huh-7, MHCC-97H and MHCC-97L, and the human normal hepatocyte, THLE2, were purchased from The Cell Bank Type Culture Collection of The Chinese Academy of Sciences. All cells were cultured in DMEM high glucose medium (Gibco; Thermo Fisher Scientific, Inc.) with 10% fetal bovine serum (FBS; Gibco; Thermo Fisher Scientific, Inc.). Cells were cultured in a closed incubator with a constant temperature of 37°C and with 5% CO₂.

Cell transfection. USP35 and PKM2 (In-PKM2) overexpressing lentiviruses were constructed using the lentiviral vector pCDH-EF1α-MCS-T2A-Puro (cat. no. CD527A-1; System Biosciences, LLC). The 3rd generation system was used and DNA was transfected into 293T cells (The Cell Bank Type Culture Collection of The Chinese Academy of Sciences) for 48 h at 37°C. The ratio used for the lentivirus, packaging and envelope plasmids was 4:3:1. For transduction, 4 μl of lentivirus titer (1x10⁸ TU/ml) was added to 1x10⁶ HCC cells at 37°C for 12 h and at three infection gradients (MOI=10, MOI=20, MOI=30). The time interval between transfection and subsequent experiments was 3 h. For the negative control (NC) group, empty vector was used instead of the overexpression vector.

Short hairpin RNA (shRNA) targeting USP35 for knockdown (De-USP35; 5'-GCTGAGTTGGGCTCTTCTAGA-3') and the respective NC (5'-TTCTCCGAACGTGTCACGTAA-3') (vector set cat. no. C01001) were purchased from Shanghai GenePharma Co., Ltd. A total of 5 μg of each plasmid was transfected into HCC cells using Lipofectamine® 3000 (Invitrogen; Thermo Fisher Scientific, Inc.) for 48 h at 37°C. The time interval between transfection and subsequent experiments was 3 h. For co-transfection, the cell lines transfected with De-USP35 were selected using 400 μg/ml geneticin. These stable cell lines were then transfected with In-PKM2, followed by selection using 2.5 μg/ml puromycin. Finally, western blotting was used to validate the results.

Western blotting. Total protein from the HCC samples from patients and cell lines was extracted in a solution of RIPA buffer (cat. no. P0013B; Beyotime Institute of Biotechnology) containing 1:100 PMSF (Beyotime Institute of Biotechnology). The protein concentration was quantified using a BCA kit (Beyotime Institute of Biotechnology) according to the manufacturer's protocol. Equal amounts of protein (25 μg) were separated via SDS-PAGE on a 10% gel and transferred to PVDF membranes. The membranes were blocked for 1 h at room temperature with 5% non-fat milk powder (Beyotime Institute of Biotechnology). The membranes were incubated at 4°C overnight with the following primary antibodies: USP35 (1:2,000; cat. no. PA5-37232; Thermo Fisher Scientific, Inc.),

PKM2 (1:1,500; cat. no. 15822-1-AP; Proteintech Group, Inc.), PKM1 (1:1,500; cat. no. 15821-1-AP; Proteintech Group, Inc.) and β -actin (1:5,000; cat. no. ab8226; Abcam). The membranes were then incubated with the appropriate HRP secondary antibodies (1:5,000; cat. nos. bs-0296G-HRP and bs-0295G-HRP; BIOSS) for 1 h at room temperature. Finally, protein expression was visualized using chemiluminescence reagents (Hyperfilm ECL; Cytivia). ImageJ software (V1.8.0.112; National Institutes of Health) was used to analyze the western blot results.

Immunohistochemistry. A total of 96 HCC tissues were fixed in 10% formalin for 12 h at room temperature, embedded in paraffin and cut into 4- μ m sections. The tissue sections were then used to generate tissue microarray cores (1.5-mm diameter). Tissue sections (slice thickness, 4 μ m) were dehydrated in xylene and alcohol followed by 3% H_2O_2 for 30 min at 37°C. All sections were incubated for 15 min at room temperature with 5% goat serum (OriGene Technologies, Inc.) to block non-specific binding, followed by incubation with USP35 (1:500; cat. no. ab254939; Abcam) and Ki-67 (1:1,000; cat. no. ab15580; Abcam) at 4°C overnight. Then, the sections incubated with anti-rabbit secondary IgG antibody (1:100; cat. no. SAP-9100; OriGene Technologies, Inc.) at 37°C for 30 min. Signals were visualized using DAB (Boster Biological Technology). Slides were visualized using a light microscope (magnification, x10, x100 or x200; Zeiss AG) and ImageJ software (version 1.52; National Institutes of Health).

The immunohistochemistry scoring method was as follows: The staining intensity score [according to the degree of color development of the positive marker: No staining, negative (score, 0); light yellow staining, weak (score, 1); brown-yellow staining, moderate (score, 2); and brown-black staining, strong (score, 3)] plus the percentage of positive cells score (score 0, \leq 5%; score 1, 6-25%; score 2, 26-50%; score 3, 51-75%; and score 4, 76-100%). USP35 expression was defined as low (total score <4) or high (total score ≥ 4).

Co-immunoprecipitation (Co-IP). Cells were collected and lysed using RIPA lysis buffer containing 1:100 PMSF (Beyotime Institute of Biotechnology). In total, 3 μ g USP35 (1:5,000; cat. no. PA5-37232; Thermo Fisher Scientific, Inc.) or PKM2 (1:500; cat. no. 15822-1-AP; Proteintech Group, Inc.) antibody was added to the lysate (20 μ l) and the mix was incubated overnight at 4°C. Then, 20 μ l Protein A/G PLUS-Agarose beads (cat. no. sc-2003; Santa Cruz Biotechnology, Inc.) was added to the lysate mix, which was incubated with rotation for 4 h at 4°C. The bead-antibody-protein complexes were washed with pre-cooled PBS solution three times and then boiled (10,000 x g centrifugation for 5 sec at room temperature) for subsequent western blot analysis.

Ubiquitination assay. Prior to cell lysis, HCC cells were treated with MG132 (10 μ M) for 8 h at 37°C. MG132 is a protease inhibitor that can prevent protease activity during degradation, thereby promoting the ubiquitination process (17). HCC cell lines were then lysed in 1% SDS-containing RIPA buffer by sonication (20 KHz, 60 sec) on ice. Then, lysates (20 μ l) were treated with Protein A/G Plus-Agarose for 1 h at room temperature. After that, each sample was incubated with 10 μ l

IgG (cat. no. 30000-0-AP; Proteintech Group, Inc.) and PKM2 (cat. no. 15822-1-AP; Proteintech Group, Inc.) overnight at 4°C. Then, the nuclear pellet was collected by centrifugation at 10,000 x g for 5 min at 4°C and subsequently washed four times with Protein A/G Plus-Agarose beads to purify the protein (this was achieved by absorbing the protein on the beads, then washing the beads to release the protein). The purified proteins were separated by 10% SDS-PAGE. An anti-PKM2 (1:500; cat. no. ab137852; Abcam) or anti-ubiquitin antibody (1:500; cat. no. ab7780; Abcam) was used for immunoblotting according to the protocol for western blotting analysis aforementioned.

The Cancer Genome Atlas (TCGA)-LIHC data acquisition and analysis. The TCGA-LIHC RNA sequencing file of expression data (from TCGA database) was downloaded from the XENA website (<http://xena.ucsc.edu/download-data/>) and the proteomic data of HBV-HCC patients was acquired from the Clinical Proteomic Tumor Analysis Consortium database (CPTAC; <https://pdc.cancer.gov/pdc/>). The expression of USP35 was selected and analyzed. Paired Student's t-test was used to compare USP35 expression in HCC and adjacent tissues using GraphPad software (V8.0.0; Dotmatics).

5-Ethynyl-2'-deoxyuridine (EdU) assay. After transfection, HCC cells (2.5×10^4 cells/well) were seeded into 96-well plates and cultured for 24 h at 37°C. Then, EdU (50 μ M) was incubated with the cells for 2 h at 37°C. Following this, the cells were fixed in 4% formaldehyde for 30 min at room temperature and then permeabilized with 0.5% Triton X-100 solution for 10 min at room temperature. ApolloR reaction cocktail (100 μ l; cat. no. 100T; Guangzhou RiboBio Co., Ltd.) was added, and the reaction was allowed to proceed for 30 min at room temperature in the dark. Cell nuclei were stained by adding 1X DAPI (100 μ l; cat. no. 100T; Guangzhou RiboBio Co., Ltd.) for 30 min at room temperature. Cell proliferation was analyzed using the mean number cells in three fields for each sample. Cell proliferation was analyzed by assessing the percentage of EdU⁺ cells in each sample using a fluorescence microscope (Lionheart; BioTek Instruments, Inc.; magnification, x100). ImageJ software (version 1.8.0; National Institutes of Health) was used for cell counting.

Cell migration and invasion assays. Transwell chambers (Corning, Inc.) were used to evaluate cell invasion with inserts precoated with Matrigel (1 mg/ml) at 37°C for 30 min. After transfection, HCC cells were resuspended in high-glucose DMEM containing 1% FBS and seeded into the upper Transwell chamber at a density of 1×10^5 cells/well and 500 μ l of high-glucose DMEM containing 10% FBS was added to the corresponding lower chamber. For the migration assay, Transwell chambers (Corning, Inc.) without inserts precoated with Matrigel were used, otherwise the same protocol as for the invasion assay was followed. After incubation for 48 h at 37°C, the Transwell chambers were fixed with 4% paraformaldehyde at room temperature for 30 min and stained with 0.5% crystal violet at room temperature for 20 min. Finally, six fields were randomly selected, the number of stained cells in the lower chamber was counted manually in each field and images were captured under a light microscope (magnification, x200; Olympus Corporation).

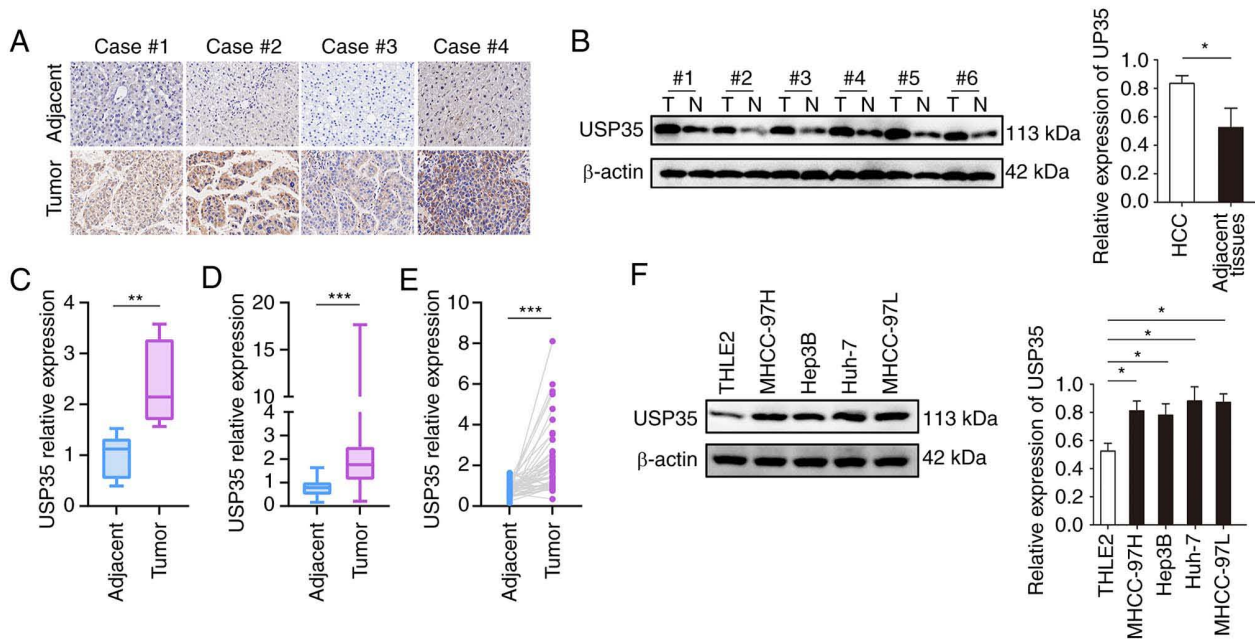


Figure 1. USP35 is highly expressed in HCC. (A) USP35 expression in HCC samples. (B) The protein expression of USP35 in HCC samples detected by western blotting. (C) The protein expression of USP35 in HCC samples from the Clinical Proteomic Tumor Analysis Consortium database. (D) USP35 protein expression in HCC samples from TCGA database (374 cases of tumor tissue and 50 cases of adjacent tissue). (E) USP35 protein expression in HCC samples from TCGA (50 cases of tumor tissue and 50 cases of adjacent tissue). (F) USP35 protein expression in HCC cell lines. * $P < 0.05$, ** $P < 0.01$, *** $P < 0.001$. HCC, hepatocellular carcinoma; N, normal (tissue); T, tumor (tissue); TCGA, The Cancer Genome Atlas database; USP35, ubiquitin-specific protease 35.

Flow cytometric analysis of apoptosis. After transfection, HCC cells were seeded into 6-well plates. At 60-70% confluency, cells were collected and incubated with Annexin V-FITC (5 μ l; Biogot Technology Co., Ltd.) and propidium iodide solution (5 μ l; Biogot Technology Co., Ltd.) at room temperature for 15 min according to the manufacturer's instructions. Cells were subsequently resuspended in 300 μ l binding buffer (cat. no. BD0073-2; Biogot Technology Co., Ltd.). Apoptosis progression was analyzed using flow cytometry (FACSaria; BD Biosciences). All data were analyzed with ModFit version 4.0 (Verity Software House, Inc.).

Glucose uptake assay. After transfection, HCC cells (1×10^5 cells/well) were incubated in DMEM (supplemented with 10% FBS) without L-glucose or phenol red (Gibco; Thermo Fisher Scientific, Inc.) for 8 h at 37°C. The D-glucose content of the medium was measured using a Glucose Colorimetric Assay kit (cat. no. K606-100; BioVision, Inc.). In total, three biological replicates were performed.

Intracellular pyruvate, lactate and ATP assays. After transfection, HCC cells (1×10^5 cells/well) were incubated in phenol red-free DMEM without FBS for 4 h at 37°C. Then, a pyruvate assay kit (cat. no. BC2205; Beijing Solarbio Science & Technology Co., Ltd.), lactate assay kit (cat. no. BC2235; Beijing Solarbio Science & Technology Co., Ltd.), and ATP assay kit (cat. no. BC0300; Beijing Solarbio Science & Technology Co., Ltd.) were used to measure intracellular concentrations of pyruvate, lactate and ATP, respectively, according to the kit manufacturer's instructions. Relative absorbance (450 nm) was measured using a spectrophotometer (Thermo Fisher Scientific, Inc.). The pyruvate, lactate and ATP contents were calculated according to the product manual.

Mouse xenograft model. Male BALB/c-nu mice ($n=12$; age, 5 weeks old; weight, 20-25 g) were purchased from Chengdu Dossy Experimental Animals Co., Ltd. and housed (25°C and 40-70% humidity, with a 12-h light/dark cycle and free access to food and water) at the Experimental Animal Center of West China Hospital of Sichuan University (Chengdu, China). All animal experiments were approved by The Committee on The Ethics of Animal Experiments of West China Hospital of Sichuan University (Chengdu, China; approval no. 20220228036). Specifically, HCC cells (5×10^6 , 50 μ l) were subcutaneously injected into the left hip flanks of the mice ($n=3$ in each group). The health and behavior of the mice was monitored once a day and the tumor growth was measured once every 4 days with a caliper. Tumor volume was then calculated according to the following formula: $\text{Volume} = (\text{width}^2 \times \text{length}) / 2$. The mice were euthanized, and tumors were collected for analysis 28 days after cell injection. For this, the mice were anesthetized with 1% pentobarbital sodium (45 mg/kg, intraperitoneal) and subsequently euthanized by cervical dislocation (it was determined that the mouse had died when the heart stopped beating completely). Body weight loss $>20\%$ was considered a humane endpoint for euthanasia, but no mice reached this humane endpoint.

Statistical analysis. All data are presented as the mean \pm SD. Statistical analysis of data was conducted using GraphPad version 5.0 (Dotmatics) or SPSS 22.0 software (IBM Corp.). Kaplan-Meier analysis was used to assess overall survival (OS) and recurrence-free survival (RFS) times, and the log-rank test was used to analyze the differences between the survival times. The relationships between USP35 expression and clinicopathological parameters in HCC was analyzed using χ^2 test. Univariate and multivariate Cox regression analyses

Table I. Associations between USP35 and the clinicopathological features of patients with HCC.

Clinicopathological feature	Cases, n	USP35 expression		P-value
		Low (n=58)	High (n=38)	
Sex				0.560
Male	49	31	18	
Female	47	27	20	
Age, years				0.734
<50	45	28	17	
≥50	51	30	21	
AFP, ng/ml				0.501
≤20	29	19	10	
>20	67	39	28	
HBsAg				0.525
Positive	62	36	26	
Negative	34	22	12	
TNM stage				0.016
I/II	46	22	24	
III/IV	50	36	14	
Tumor size, cm				0.507
≤5	44	25	19	
>5	52	33	19	
Multiplicity				0.012
Single	48	23	25	
≥2	48	35	13	
Microvascular invasion				0.006
Presence	44	20	24	
Absence	52	38	14	

AFP, α-fetoprotein; HBsAg, hepatitis B surface antigen; TNM, tumor-node-metastasis.

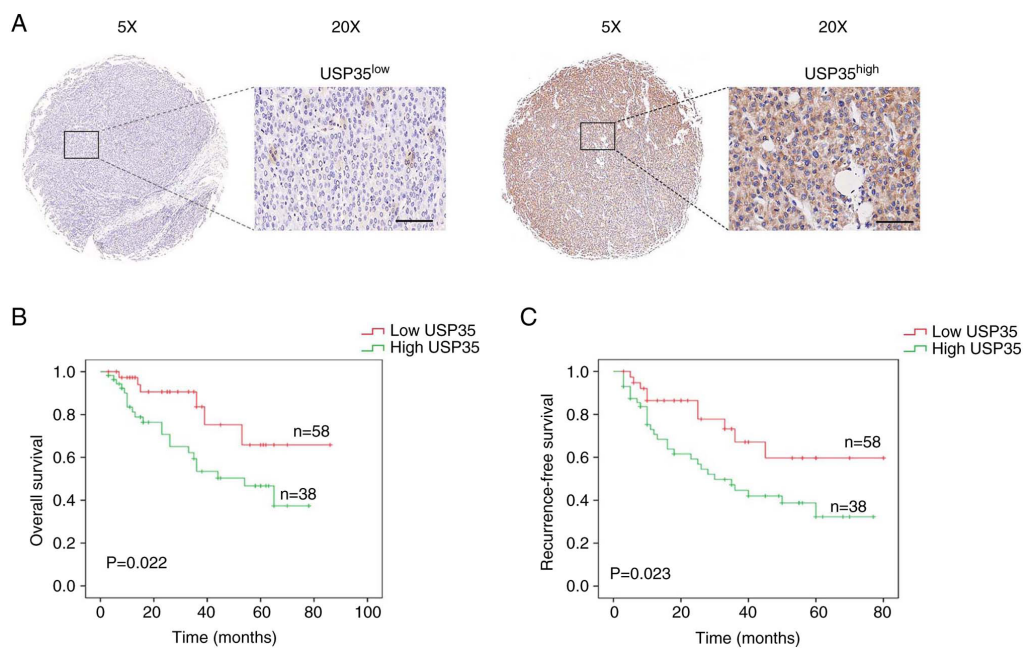


Figure 2. Relationship between USP35 expression and prognosis of patients with hepatocellular carcinoma. (A) Representative immunohistochemistry images of high and low USP35 expression. (B) Kaplan-Meier analysis of overall survival. (C) Kaplan-Meier analysis of recurrence-free survival. USP35, ubiquitin-specific protease 35.

Table II. Univariate and multivariate analysis of different prognostic variables influencing overall survival in patients with HCC.

Variables	n	Univariate analysis		Multivariate analysis	
		HR (95% CI)	P-value	HR (95% CI)	P-value
Sex		0.534 (0.345-1.833)	0.421		
Male	49				
Female	47				
Age, years		0.593 (0.487-1.931)	0.547		
<50	45				
≥50	51				
AFP, ng/ml		1.634 (0.208-1.307)	0.364		
≤20	29				
>20	67				
HBsAg		1.744 (0.813-3.175)	0.364		
Positive	62				
Negative	34				
TNM stage		1.117 (0.314-1.311)	0.017	1.174 (0.297-1.473)	0.005
I/II	46				
III/IV	50				
Tumor size, cm		0.637 (0.740-1.942)	0.471		
≤5	44				
>5	52				
Multiplicity		1.394 (0.471-1.634)	0.520		
Single	48				
≥2	48				
Microvascular invasion		1.438 (0.604-1.976)	0.023	1.307 (0.573-1.864)	0.010
Presence	44				
Absence	52				
USP35 expression		1.084 (0.519-1.843)	0.011	1.128 (0.619-1.784)	0.013
Low	58				
High	38				

AFP, α-fetoprotein; HBsAg, hepatitis B surface antigen; CI, confidence interval; HR, hazard ratio; TNM, tumor-node-metastasis.

were conducted to determine the prognostic value of USP35. Statistical differences between two groups were analyzed by unpaired Student's t-test. Paired Student's t-test was used to compare USP35 expression in HCC and adjacent tissues. ANOVA was used for multiple group comparisons and Tukey's test was used as the post hoc test after ANOVA. $P < 0.05$ was considered to indicate a statistically significant difference.

Results

USP35 is upregulated in HCC and predicts poor prognosis. Firstly, the expression of USP35 in paired HCC tumor and adjacent tissues was detected by immunohistochemistry. As shown in Fig. 1A, USP35 was highly expressed in tumor tissues, which was further verified by western blotting (Fig. 1B). In addition, the mRNA level of USP35 in the HBV-HCC cohort from the CPTAC (Fig. 1C) and the TCGA-LIHC cohort from TCGA (Fig. 1D and E) were analyzed, and it was found that USP35 mRNA was highly expressed in tumor tissues. The

western blot results also demonstrated that USP35 was significantly upregulated in HCC cell lines compared with THLE2 normal liver cells (Fig. 1F).

To evaluate the expression of USP35, tissue microarray was used. The 96 patients with HCC were clustered into two groups, the USP35 low and USP35 high groups, based on USP35 expression scored by the positive rate and staining intensity (Fig. 2A). Furthermore, the association between USP35 expression and clinical parameters were evaluated. As demonstrated in Table I, USP35 expression was associated with Tumor-Node-Metastasis (TNM) stage ($P = 0.016$) [using the Barcelona Clinic Liver Cancer 2022 strategy (18)], microvascular invasion ($P = 0.006$) and multiplicity ($P = 0.012$). Statistical analysis of prognosis revealed that patients with HCC with higher USP35 expression had a significantly shorter overall survival time (Fig. 2B). Univariate analysis indicated that TNM stage ($P = 0.017$), microvascular invasion ($P = 0.023$) and USP35 ($P = 0.011$) were significantly associated with OS time in HCC (Table II). In addition, statistical

Table III. Univariate and multivariate analysis of different prognostic variables influencing recurrence-free survival in patients with HCC.

Variables	n	Univariate analysis		Multivariate analysis	
		HR (95% CI)	P-value	HR (95% CI)	P-value
Sex		0.237 (0.648-1.178)	0.348		
Male	49				
Female	47				
Age, years		0.573 (0.710-1.686)	0.513		
<50	45				
≥50	51				
AFP, ng/ml		0.713 (0.422-1.571)	0.484		
≤20	29				
>20	67				
HBsAg		1.517 (0.847-1.870)	0.348		
Positive	62				
Negative	34				
TNM stage		1.109 (0.506-1.811)	0.014	1.277 (0.594-2.033)	0.022
I/II	46				
III/IV	50				
Tumor size, cm		0.814 (0.664-1.734)	0.439		
≤5	44				
>5	52				
Multiplicity		1.027 (0.476-1.974)	0.604		
Single	48				
≥2	48				
Microvascular invasion		1.008 (0.307-1.738)	0.010	1.114 (0.411-1.488)	0.015
Presence	44				
Absence	52				
USP35 expression		1.375 (0.705-1.881)	0.012	1.512 (0.880-1.947)	0.015
Low	58				
High	38				

AFP, α-fetoprotein; HBsAg, hepatitis B surface antigen; CI, confidence interval; HR, hazard ratio; TNM, tumor-node-metastasis.

analysis of prognosis revealed that patients with HCC with higher USP35 expression had a significantly shorter RFS time (Fig. 2C). Univariate analysis indicated that TNM stage (P=0.014), microvascular invasion (P=0.010) and USP35 (P=0.012) were significantly associated with RFS time in HCC (Table III).

Decreased USP35 expression inhibits the malignant biological behavior of HCC. Loss-of-function experiments were performed in Huh-7 and Hep3B cells. The expression of USP35 was effectively knocked down in Huh-7 and Hep3B cells (Fig. 3A and B, respectively). Decreased USP35 expression significantly inhibited cell proliferation, as demonstrated by the EdU assays in Huh-7 and Hep3B cells (Fig. 3C and D, respectively). The results from flow cytometry assays demonstrated that decreased USP35 expression elevated the apoptosis rate of Huh-7 (1.5 vs. 10.1%; Fig. 3E) and Hep3B (1.1 vs. 6.2%; Fig. 3F) cells. Moreover, the migration and invasion abilities

of Huh-7 and Hep3B cells with decreased USP35 expression were significantly impaired, as determined by Transwell assays (Fig. 3G-J).

Decreased USP35 expression impedes energy metabolism by suppressing glycolysis in HCC. The liver is the main organ in which glucose and lipid metabolism occurs in the body. After the occurrence of liver cancer, the normal metabolism of glucose and lipids *in vivo* markedly changes (19). USP35 subtype 2 is an integral membrane protein of the endoplasmic reticulum and is also present in lipid droplets (20). Dysregulation of the level of subtype 2 may lead to rapid endoplasmic reticulum stress and cell death by interfering with the regulation of lipid homeostasis (20). In the present study, it was investigated whether USP35 affects glycolysis in HCC. It was found that glucose uptake and the production of ATP, pyruvate and lactate were significantly decreased after USP35 downregulation in Huh-7 cells (Fig. 4A-D). Similarly, it was

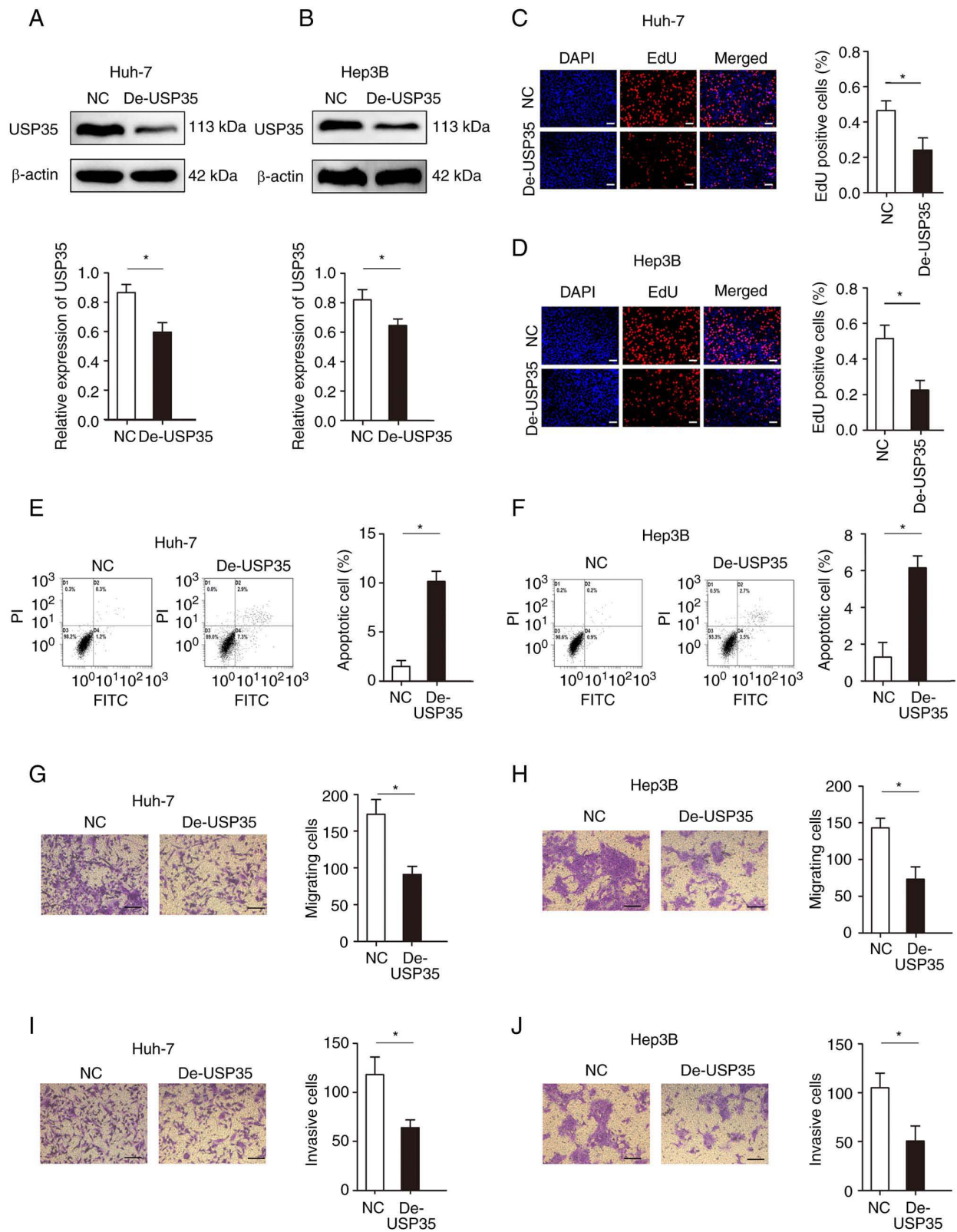


Figure 3. Decreased USP35 expression inhibits the malignant biological behavior of hepatocellular carcinoma cells. USP35 protein expression in (A) Huh-7 and (B) Hep3B cell lines. EdU incorporation assays were used to analyze the effect of USP35 on (C) Huh-7 and (D) Hep3B cell proliferation (scale bars, 50 μ m). The effect of USP35 on the apoptosis of (E) Huh-7 and (F) (Hep3B) cells. Transwell assays were performed to determine the effects of USP35 on (G) Huh-7 and (H) Hep3B migration and (I) Huh-7 and (J) Hep3B invasion (scale bars, 100 μ m). * P <0.05. Edu, 5-ethynyl-2'-deoxyuridine; NC, negative control; USP35, ubiquitin-specific protease 35; De-USP35, USP35 short hairpin RNA.

demonstrated that glucose uptake and the production of ATP, pyruvate and lactate were significantly decreased upon USP35 downregulation in Hep3B cells (Fig. 4E-H).

USP35 binds to PKM2 and regulates PKM2 expression through ubiquitination in HCC. In the process of glycolysis, PKM1 and PKM2 convert phosphoenolpyruvate into pyruvate

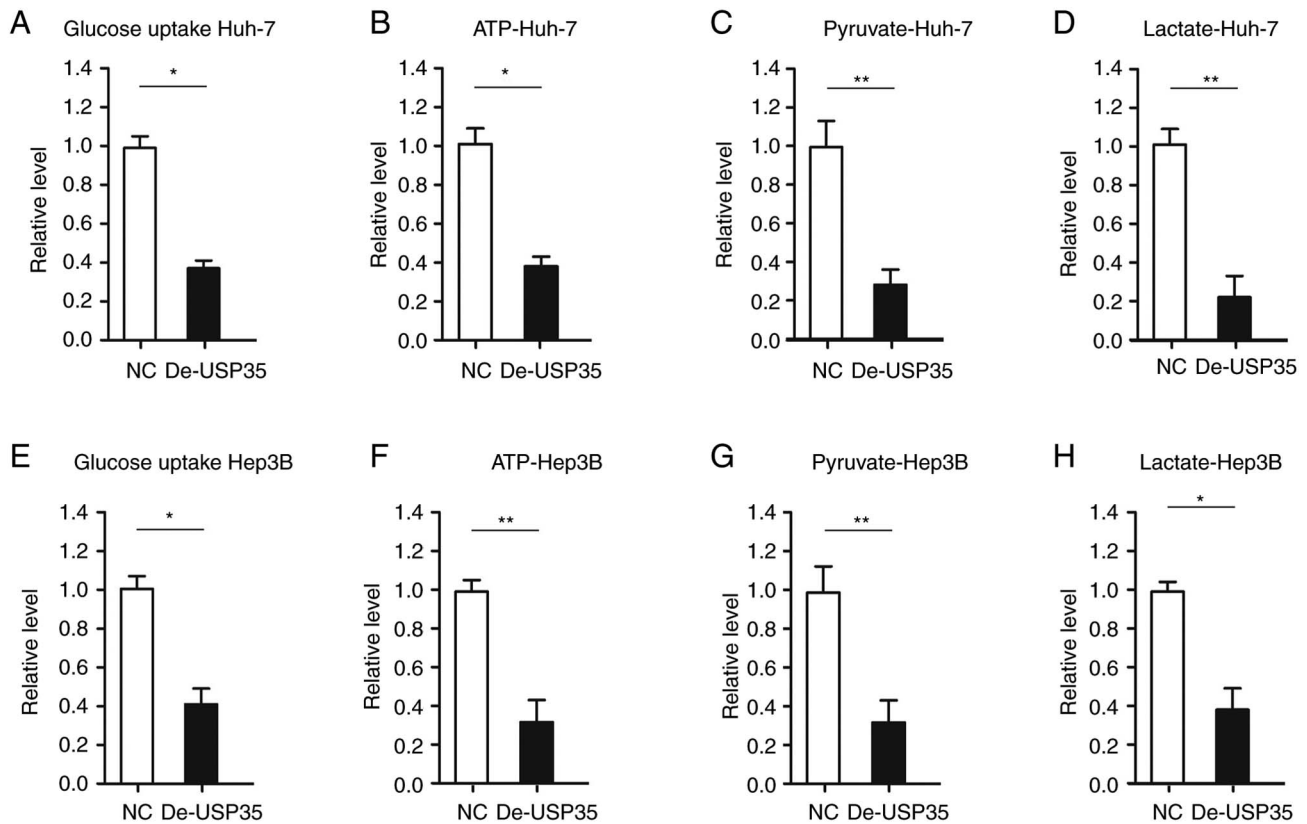


Figure 4. USP35 regulates the energy metabolism of hepatocellular carcinoma cells. The effects of USP35 on (A) glucose uptake and the (B) ATP, (C) pyruvate and (D) lactate levels of Huh-7 cells. The effects of USP35 on (E) glucose uptake and the (F) ATP, (G) pyruvate and (H) lactate levels of Hep3B cells. * $P < 0.05$, ** $P < 0.01$. NC, negative control; USP35, ubiquitin-specific protease 35; De-USP35, USP35 short hairpin RNA.

and play critical roles in regulating the glycolysis process (21). Therefore, in the present study, the association of USP35 expression with that of PKM1 and PKM2 were analyzed. It was found that changing the expression level of USP35 did not affect the expression of PKM1 (Fig. 5A and B). However, PKM2 displayed a similar expression pattern to USP35 in HCC tissues (for example, when USP35 was highly expressed, PKM2 was also highly expressed; Fig. 5C). In addition, overexpression of USP35 significantly increased the expression of PKM2, while knock down of USP35 expression significantly decreased the expression of PKM2 (Fig. 6A and B). Notably, the Co-IP assay results indicated the existence of an interaction between endogenous USP35 and PKM2 (Fig. 6C and D). In addition, the ubiquitination level of PKM2 was decreased in the Huh-7 and Hep3B cell lines after USP35 overexpression, which indicated that overexpression of USP35 inhibits PKM2 from entering the degradation process (Fig. 6E and F).

PKM2 ameliorates the inhibitory effect of USP35 on HCC progression. Furthermore, rescue experiments were performed to investigate whether PKM2 in HCC was mediated by USP35. PKM2 expression was significantly increased when overexpressed in Huh and Hep3B (Fig. S1), and significantly increased when overexpressed in Huh-7-De-USP35 and Hep3B-De-USP35 (Fig. 7A and B). EdU assays demonstrated that PKM2 overexpression significantly abolished the inhibitory effects of USP35 knockdown on proliferation (Fig. 7C and D). Moreover, increased PKM2 expression significantly decreased the inhibitory effect of USP35 knockdown on migration and

invasion in Huh-7-De-USP35 and Hep3B-De-USP35 cells (Fig. 7E-H). In addition, PKM2 overexpression significantly rescued the inhibitory effects of USP35 knockdown on tumor growth *in vivo* (Fig. 7I and J).

Furthermore, considering the role of PKM2 in glycolysis, the effect of PKM2 on energy metabolism in HCC was examined. It was found that increased PKM2 expression significantly abolished the inhibitory effects of USP35 knockdown on glucose uptake in Huh-7-De-USP35 and Hep3B-De-USP35 cells (Fig. 8A and E). Additionally, the results indicated that the levels of pyruvate and lactate, and the production of ATP were all significantly increased after increasing of PKM2 expression in Huh-7-De-USP35 and Hep3B-De-USP35 (Fig. 8B-D and Fig. 8F-H, respectively).

Discussion

The ubiquitin-proteasome pathway is one of the important components in the regulatory system of protein degradation (22). Through the multiubiquitination of substrate proteins and the degradation by proteasomes, various biological processes of intracellular proteins are regulated, such as the expression of proteins after gene transcription, regulation of cell growth cycle, immune response, tumorigenesis and development (22). The ubiquitin-proteasome pathway is also a dynamic and reversible protein modification process. The protein substrate in the cell is ubiquitinated by the ubiquitin ligase system (E1-E2-E3) (23). In addition, the DUB family removes ubiquitin molecules from ubiquitin-modified proteins

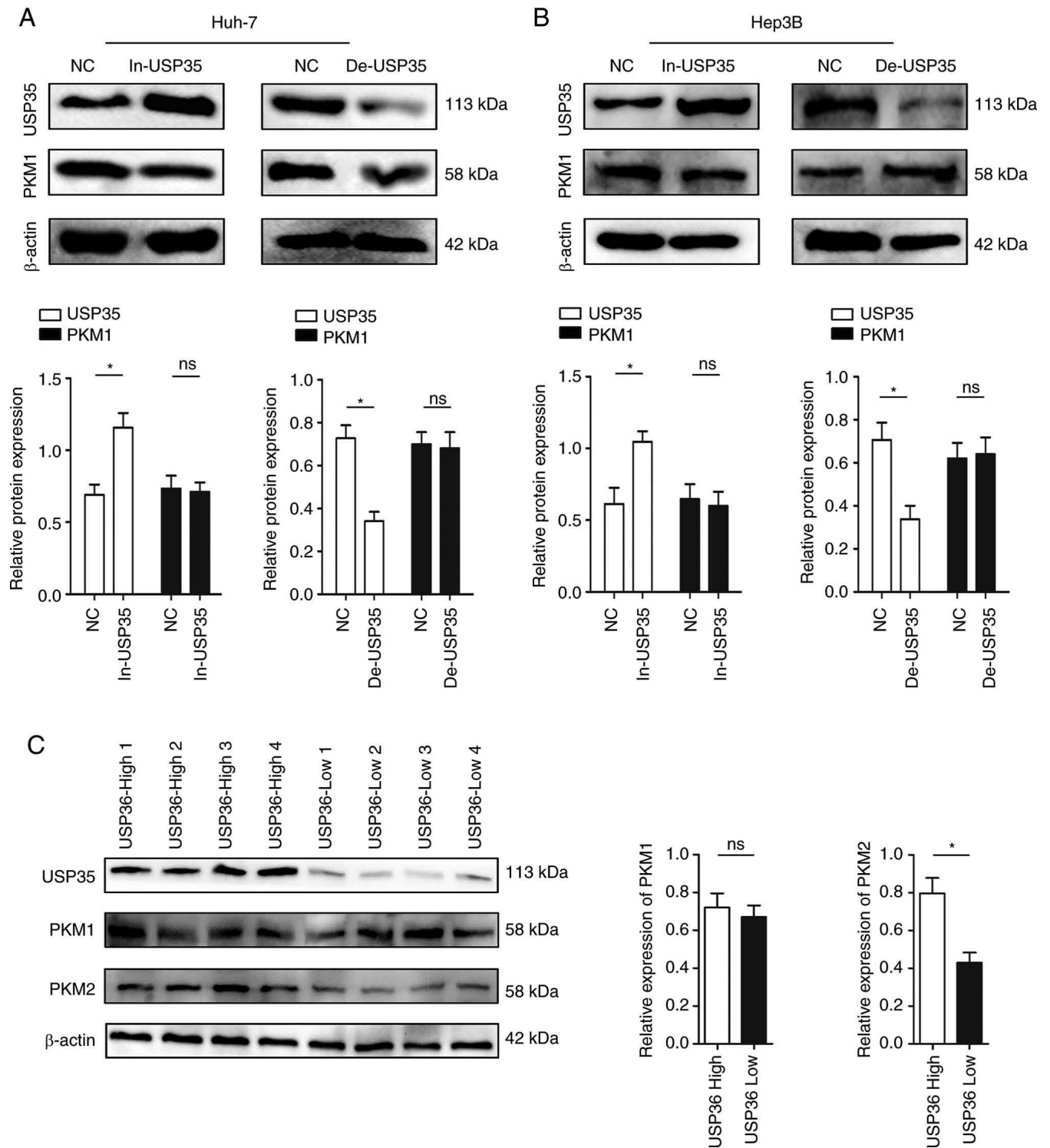


Figure 5. Expression of PKM1 and PKM2 in HCC cells following USP35 overexpression or knockdown. (A) USP35 and PKM1 protein expression in Huh-7 cells transfected with In-USP35 or De-USP35. (B) USP35 and PKM1 protein expression in Hep3B cells transfected with In-USP35 or De-USP35. (C) USP35, PKM1 and PKM2 protein expression levels in hepatocellular carcinoma samples. * $P < 0.05$. ns, not significant; NC, negative control; PKM1/2, M1/2 splice isoform of pyruvate kinase; USP35, ubiquitin-specific protease 35; De-USP35, USP35 short hairpin RNA; In-USP35, USP35 overexpression.

by hydrolyzing ester, peptide or isopeptide bonds at the carboxyl end of ubiquitin. Members of the DUB family play a key role in protein deubiquitination and are involved in various physiological and pathological processes, such as malignant growth and proliferation of tumors, inflammatory responses and the immune response (23). The functions of DUBs in cells can be broadly divided into the following categories: i) Processing

ubiquitin precursors to produce free ubiquitin molecules; ii) removing a ubiquitin chain on a protein to prevent the protein from being degraded by the proteasome, thereby stabilizing the protein; iii) removing the non-degradable ubiquitination signal attached to a protein; iv) ensuring the homeostasis of ubiquitin molecules in cells by preventing ubiquitin molecules from being degraded with substrate proteins; v) participating

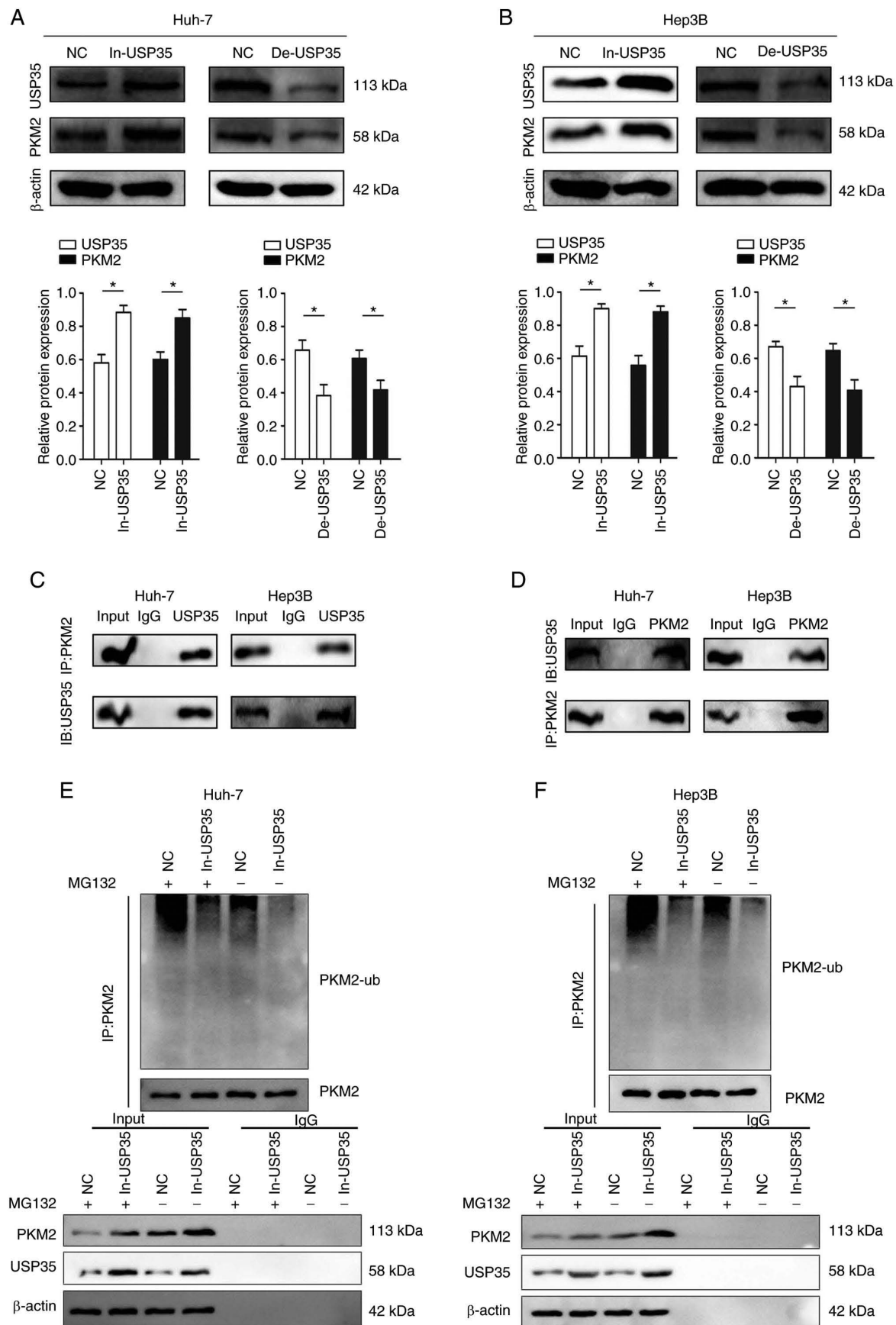


Figure 6. USP35 regulates PKM2 expression by influencing its ubiquitin level. USP35 and PKM2 protein expression in (A) Huh-7 and (B) Hep3B cells transfected with In-USP35 or De-USP35. (C) Co-IP experiments indicated that USP35 interacted with PKM2 in Huh-7 and Hep3B cell lines (IP:PKM2, IB:USP35). (D) Co-IP experiments indicated that USP35 interacted with PKM2 in Huh-7 and Hep3B cell lines (IP:USP35, IB:PKM2). The levels of PKM2-ub in (E) Huh-7 and (F) Hep3B cells following overexpression of USP35 were examined by western blotting using an anti-ubiquitin antibody. * $P < 0.05$. Co-IP, co-immunoprecipitation; NC, negative control; PKM2, M2 splice isoform of pyruvate kinase; PKM2-ub, PKM2 ubiquitination; USP35, ubiquitin-specific protease 35; De-USP35, USP35 short hairpin RNA; In-USP35, USP35 overexpression; IB, immunoblotting.

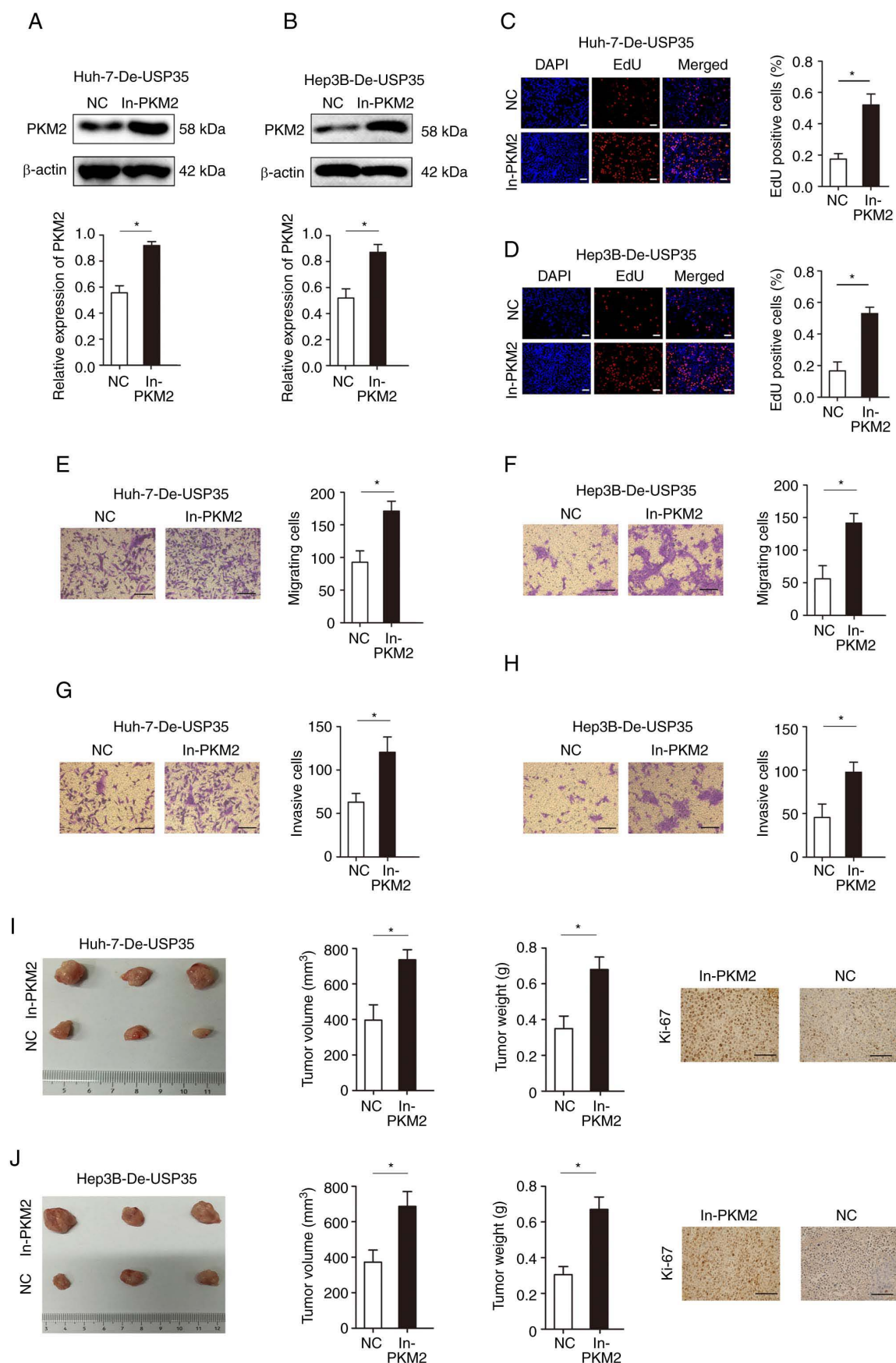


Figure 7. USP35 regulates the malignant biological behavior of hepatocellular carcinoma through PKM2. PKM2 protein expression in USP35 knockdown (A) Huh7 and (B) Hep3B cell lines, following PKM2 overexpression. EdU incorporation assays were used to analyze the effect of PKM2 overexpression on (C) Huh-7-DeUSP35 and (D) Hep3B-De-USP35 cell proliferation (scale bars, 50 μ m). The effects of PKM2 on (E) Huh-7-De-USP35 and (F) Hep3B-De-USP35 migration and (G) Huh-7-De-USP35 and (H) Hep3B-De-USP35 invasion (scale bars, 100 μ m). The effects of PKM2 overexpression on (I) Huh-7-DeUSP35 and (J) Hep3B-De-USP35 tumor formation *in vivo*. * $P < 0.05$. Edu, 5-ethynyl-2'-deoxyuridine; NC, negative control; PKM2, M2 splice isoform of pyruvate kinase; In-PKM2, PKM2 overexpression; De-USP35, ubiquitin-specific protease 35 short hairpin RNA.

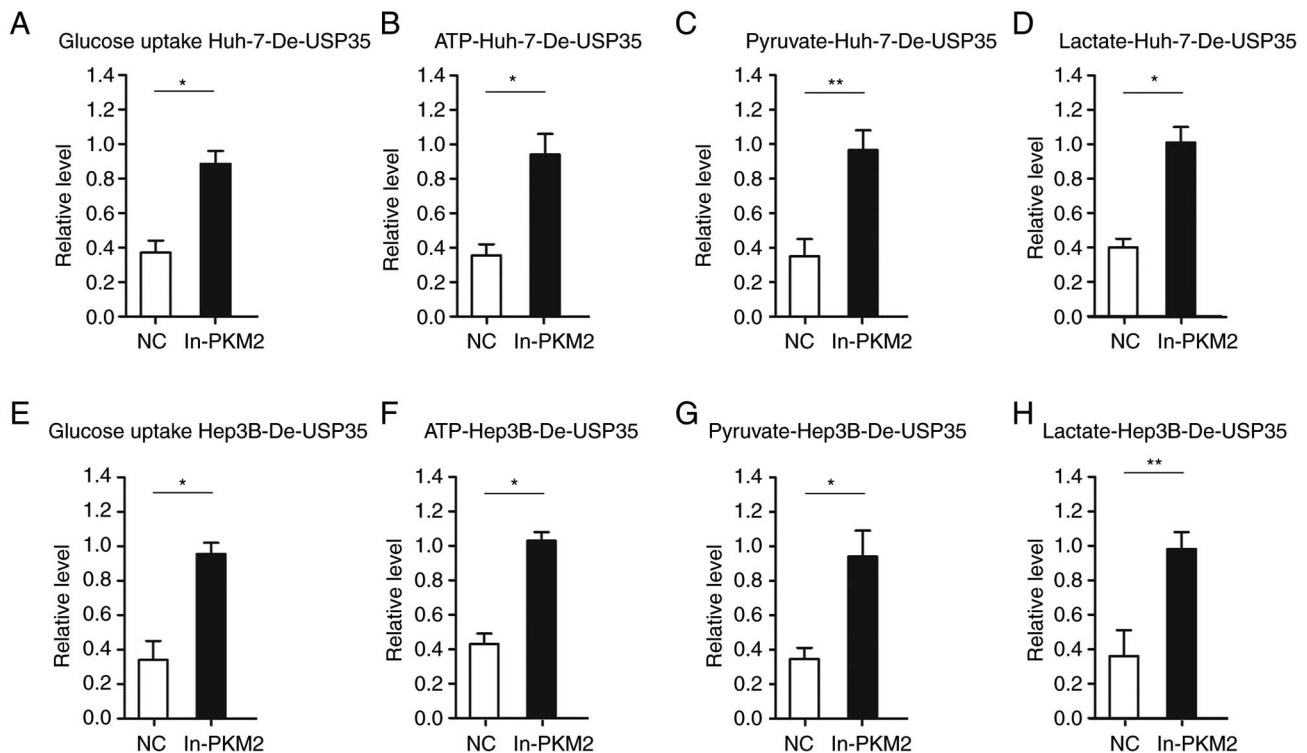


Figure 8. USP35 regulates energy metabolism of hepatocellular carcinoma cells through PKM2. The effects of PKM2 overexpression on (A) glucose uptake and (B) ATP, (C) pyruvate and (D) lactate levels of Huh-7-De-USP35 cells. The effects of PKM2 overexpression on (E) glucose uptake and (F) ATP, (G) pyruvate and (H) lactate levels of Hep3B-De-USP35 cells. *P<0.05, **P<0.01. NC, negative control; PKM2, M2 splice isoform of pyruvate kinase; In-PKM2, PKM2 overexpression; De-USP35, ubiquitin-specific protease 35 short hairpin RNA.

in the disintegration of intracellular free ubiquitin chains; and vi) editing the type of ubiquitin chain by cutting the ubiquitin chain (22,23). USP35 plays an important role in the deubiquitination of proteins and in the regulation of tumor progression. USP35 interacts with estrogen receptor α (ER α) and enhances its stability through deubiquitination, further enhancing the transcriptional activity of ER α by interacting with ER α in the DNA region containing the estrogen response element, prompting the development of endocrine therapy for resistant ER $^{+}$ breast cancers (24). USP35 interacts directly with ribosome binding protein 1 (RRBP1) to prevent its degradation by proteolytic enzymes (25). Furthermore, USP35 attenuates endoplasmic reticulum stress-induced apoptosis by stabilizing RRBP1 in non-small cell lung cancer cells (25). In addition, USP39 participates in the deubiquitination of SP1 protein and promotes the proliferation of HCC cells in a SP1-dependent manner (26). Knockdown of USP39 can promote apoptosis and cell cycle arrest in HCC cells, and SP1 reverses these effects (26). In HCC, USP10 directly interacts with SMAD4 and stabilizes it through proteolytic cleavage of its linked ubiquitin, thereby promoting the malignant progression of HCC (27). In the present study, the results indicated that USP35 expression was increased in HCC and was associated with a poor prognosis. Effectively, decreasing the expression of USP35 may significantly inhibit the malignant biological behavior of HCC.

Normally differentiated cells mainly rely on oxidative phosphorylation in mitochondria for energy supply, while most tumor cells rely on aerobic glycolysis (28). This phenomenon is termed the Warburg effect. The efficiency of aerobic

glycolysis for ATP is very low, but it endows tumor cells more advantages, such as providing more energy and metabolic products for the rapid growth of tumors and helping to maintain cellular redox homeostasis (28). It has been found that some cancer-related mutations enable tumor cells to acquire and metabolize nutrients in a manner conducive to proliferation rather than efficient production of ATP (29). PKM2 plays a key role in the glucose metabolism of cancer cells (30). PKM2 converts phosphoenolpyruvate and ADP into pyruvate and ATP and is one of the main rate limiting enzymes in glycolysis (31,32). When the EGF receptor is activated in cells, PKM2 binds to histone H3 and phosphorylates histone H3 at T11 (33). This phosphorylation is required for the dissociation of HDAC3 from the cyclin D and Myc promoter regions and the subsequent acetylation of histone H3 at K9 (33). PKM2-dependent histone H3 modification contributes to EGF-induced cyclin D1 and c-Myc expression, promoting tumor cell proliferation, cell cycle progression and tumorigenesis (33). PKM2 translocates to mitochondria under oxidative stress in tumor cells (33). In mitochondria, PKM2 binds to and phosphorylates T69 of Bcl2 (34). This phosphorylation prevents tumor cell apoptosis by preventing Cul3-E3 ligase-based binding to Bcl2 and subsequent Bcl2 degradation. The results of the present study are consistent with a previous study where it was demonstrated that PKM2 regulates the malignant development of tumors (34). Notably, the results of the present study demonstrated that PKM2 was regulated by ubiquitination by USP35 and affected the glycolytic process in HCC through the Warburg effect (as shown by the changes in energy metabolism in HCC cells). In HCC, zinc finger protein 91 homolog promotes ubiquitination

of the oncoprotein, heterogeneous nuclear ribonucleoprotein A1, at K48 and its subsequent proteasomal degradation, and inhibits the splicing of hnRNP A1-dependent PKM (35). This in turn leads to an upregulation of PKM1 and downregulation of PKM2, inhibition of the reprogramming of glucose metabolism and the proliferation and metastasis of tumor cells (35). Rho GTPase activating protein 24 (ARHGAP24) recruits the E3 ligase, WWP1, which promotes the degradation of PKM2 and targets the ARHGAP24/WWP1/PKM2/ β -catenin axis, regulating the malignant progression of HCC (36).

The present study does have some limitations. First, the 96 clinical samples of HCC collected constituted a small study cohort. In a follow-up study, the clinical sample size will be expanded to provide a reliable clinical basis for further study of the role of USP35 in HCC. Second, regarding the animal model, USP35 liver-specific knockout mice will be used in future research to further analyze the molecular mechanisms by which USP35 affects HCC malignant progression through PKM2. Third, the patients with multinodular HCC enrolled in the present study were evaluated as being suitable for hepatectomy, with no more than three nodules, most of which were <5 cm or were even 3 cm in diameter. In this case, some patients with HCC were classified as low TNM stage or early stage. Therefore, although it seems unreasonable, it is possible for USP35 to be expressed at a low level in these patients. As patients with HCC with liver cancer nodules >3 were not included in the study, this is a deficiency of the present study.

In conclusion, the results of the present study demonstrated that USP35 was significantly elevated in HCC. USP35 regulated the PKM2 protein level through deubiquitination and affected the glycolysis process in HCC through the Warburg effect, which further regulated the malignant progression of HCC. The present study provides an objective experimental basis for further study on the role of ubiquitination and the Warburg effect in HCC and provides a scientific basis for precise treatment of HCC, from the perspective of energy metabolism.

Acknowledgements

Not applicable.

Funding

This work was supported by grants from the Natural Science Foundation of China (grant nos. 82070674, 82173255 and 82270691), the Key R&D projects of Sichuan Provincial Department of Science and Technology (grant no. 2022YFS0253), the China Postdoctoral Science Foundation Grant (grant no. 2021M702343), the 'Post-Doctor Research Project' from West China Hospital, Sichuan University (grant no. 2020HXBH133) and the 'Postdoctoral Cross Interdisciplinary Innovation Initiation Fund' from Sichuan University (grant no. 20210317).

Availability of data and materials

The datasets used and/or analyzed during the current study are available from the corresponding author on reasonable request.

Authors' contributions

TL, JY and YZ conceived and designed the study. TL, BZ, CJ and QZ performed the experiments. TL and YZ analyzed the data. TL and JY wrote the manuscript. TL, JY and YZ confirm the authenticity of all the raw data. All authors read and approved the final version of the manuscript.

Ethics approval and consent to participate

All animal experiments were approved by The Committee on The Ethics of Animal Experiments of West China Hospital of Sichuan University (Chengdu, China; approval no. 20220228036). The patient study was conducted with the approval of The Ethics Committee of West China Hospital of Sichuan University (approval no. 20150176). Written informed consent was obtained from all patients for the use of their tissue in this study.

Patient consent for publication

Not applicable.

Competing interests

The authors declare that they have no competing interests.

References

1. Couri T and Pillai A: Goals and targets for personalized therapy for HCC. *Hepatol Int* 13: 125-137, 2019.
2. Chakraborty E and Sarkar D: Emerging therapies for hepatocellular carcinoma (HCC). *Cancers (Basel)* 14: 2798, 2022.
3. Crocetti L, Bargellini I and Cioni R: Loco-regional treatment of HCC: Current status. *Clin Radiol* 72: 626-635, 2017.
4. Kulik L and El-Serag HB: Epidemiology and management of hepatocellular carcinoma. *Gastroenterology* 156: 477-491.e1, 2019.
5. De Stefano F, Chacon E, Turcios L, Marti F and Gedaly R: Novel biomarkers in hepatocellular carcinoma. *Dig Liver Dis* 50: 1115-1123, 2018.
6. Sayiner M, Golabi P and Younossi ZM: Disease burden of hepatocellular carcinoma: A global perspective. *Dig Dis Sci* 64: 910-917, 2019.
7. Fujiwara N, Friedman SL, Goossens N and Hoshida Y: Risk factors and prevention of hepatocellular carcinoma in the era of precision medicine. *J Hepatol* 68: 526-549, 2018.
8. Sahu SK, Chawla YK, Dhiman RK, Singh V, Duseja A, Taneja S, Kalra N and Gorski U: Rupture of hepatocellular carcinoma: A review of literature. *J Clin Exp Hepatol* 9: 245-256, 2019.
9. Sharma D and Mandal P: NAFLD: Genetics and its clinical implications. *Clin Res Hepatol Gastroenterol* 46: 102003, 2022.
10. Shah PA, Patil R and Harrison SA: NAFLD-related hepatocellular carcinoma: The growing challenge. *Hepatology* 77: 323-338, 2023.
11. Popovic D, Vucic D and Dikic I: Ubiquitination in disease pathogenesis and treatment. *Nat Med* 20: 1242-1253, 2014.
12. Mansour MA: Ubiquitination: Friend and foe in cancer. *Int J Biochem Cell Biol* 101: 80-93, 2018.
13. van Wijk SJ, Fulda S, Dikic I and Heilemann M: Visualizing ubiquitination in mammalian cells. *EMBO Rep* 20: e46520, 2019.
14. Komander D: The emerging complexity of protein ubiquitination. *Biochem Soc Trans* 37: 937-953, 2009.
15. Tang Z, Jiang W, Mao M, Zhao J, Chen J and Cheng N: Deubiquitinase USP35 modulates ferroptosis in lung cancer via targeting ferroportin. *Clin Transl Med* 11: e390, 2021.
16. Zhang J, Chen Y, Chen X, Zhang W, Zhao L, Weng L, Tian H, Wu Z, Tan X, Ge X, *et al*: Deubiquitinase USP35 restrains STING-mediated interferon signaling in ovarian cancer. *Cell Death Differ* 28: 139-155, 2021.

17. Zhong Q, Wang Z, Kang H and Wu R: Molecular mechanism of FBXW7-mediated ubiquitination modification in nasopharyngeal carcinoma cell proliferation in vitro and in vivo. *Pathol Res Pract* 244: 154056.2023.
18. Reig M, Forner A, Rimola J, Ferrer-Fàbrega J, Burrel M, Garcia-Criado Á, Kelley RK, Galle PR, Mazzaferro V, Salem R, *et al*: BCLC strategy for prognosis prediction and treatment recommendation: The 2022 update. *J Hepatol* 76: 681-693, 2022.
19. Beyoğlu D and Idle JR: The metabolomic window into hepatobiliary disease. *J Hepatol* 59: 842-858, 2013.
20. Leznicki P, Natarajan J, Bader G, Spevak W, Schlattl A, Abdul Rehman SA, Pathak D, Weidlich S, Zoephel A, Bordone MC, *et al*: Expansion of DUB functionality generated by alternative isoforms-USP35, a case study. *J Cell Sci* 131: jcs212753, 2018.
21. Zhang Z, Deng X, Liu Y, Liu Y, Sun L and Chen F: PKM2, function and expression and regulation. *Cell Biosci* 9: 52, 2019.
22. Sun T, Liu Z and Yang Q: The role of ubiquitination and deubiquitination in cancer metabolism. *Mol Cancer* 19: 146, 2020.
23. Liu Y and Deng J: Ubiquitination-deubiquitination in the Hippo signaling pathway (review). *Oncol Rep* 41: 1455-1475, 2019.
24. Cao J, Wu D, Wu G, Wang Y, Ren T, Wang Y, Lv Y, Sun W, Wang J, Qian C, *et al*: USP35, regulated by estrogen and AKT, promotes breast tumorigenesis by stabilizing and enhancing transcriptional activity of estrogen receptor α . *Cell Death Dis* 12: 619, 2021.
25. Wang W, Wang M, Xiao Y, Wang Y, Ma L, Guo L, Wu X, Lin X and Zhang P: USP35 mitigates endoplasmic reticulum stress-induced apoptosis by stabilizing RRBPI in non-small cell lung cancer. *Mol Oncol* 16: 1572-1590, 2022.
26. Dong X, Liu Z, Zhang E, Zhang P, Wang Y, Hang J and Li Q: USP39 promotes tumorigenesis by stabilizing and deubiquitinating SP1 protein in hepatocellular carcinoma. *Cell Signal* 85: 110068, 2021.
27. Yuan T, Chen Z, Yan F, Qian M, Luo H, Ye S, Cao J, Ying M, Dai X, Gai R, *et al*: Deubiquitinating enzyme USP10 promotes hepatocellular carcinoma metastasis through deubiquitinating and stabilizing Smad4 protein. *Mol Oncol* 14: 197-210, 2020.
28. Liberti MV and Locasale JW: The Warburg effect: How does it benefit cancer cells? *Trends Biochem Sci* 41: 211-218, 2016.
29. Pascale RM, Calvisi DF, Simile MM, Feo CF and Feo F: The Warburg effect 97 years after its discovery. *Cancers (Basel)* 12: 2819, 2020.
30. Israelsen WJ and Vander Heiden MG: Pyruvate kinase: Function, regulation and role in cancer. *Semin Cell Dev Biol* 43: 43-51, 2015.
31. Grant MM: Pyruvate kinase, inflammation and periodontal disease. *Pathogens* 10: 784, 2021.
32. Zahra K, Dey T, Ashish, Mishra SP and Pandey U: Pyruvate kinase M2 and cancer: The role of PKM2 in promoting tumorigenesis. *Front Oncol* 10: 159, 2020.
33. Yang W, Xia Y, Hawke D, Li X, Liang J, Xing D, Aldape K, Hunter T, Alfred Yung WK and Lu Z: PKM2 phosphorylates histone H3 and promotes gene transcription and tumorigenesis. *Cell* 150: 685-696, 2012.
34. Liang J, Cao R, Wang X, Zhang Y, Wang P, Gao H, Li C, Yang F, Zeng R, Wei P, *et al*: Mitochondrial PKM2 regulates oxidative stress-induced apoptosis by stabilizing Bcl2. *Cell Res* 27: 329-351, 2017.
35. Chen D, Wang Y, Lu R, Jiang X, Chen X, Meng N, Chen M, Xie S and Yan GR: E3 ligase ZFP91 inhibits hepatocellular carcinoma metabolism reprogramming by regulating PKM splicing. *Theranostics* 10: 8558-8572, 2020.
36. Yang W, Wang B, Yu Q, Liu T, Li T, Tian T, Jin A, Ding L, Chen W, Wang H, *et al*: ARHGAP24 represses β -catenin transactivation-induced invasiveness in hepatocellular carcinoma mainly by acting as a GTPase-independent scaffold. *Theranostics* 12: 6189-6206, 2020.



Copyright © 2023 Lv et al. This work is licensed under a Creative Commons Attribution-NonCommercial-NoDerivatives 4.0 International (CC BY-NC-ND 4.0) License.